Non-monotonic step-induced magnetic anisotropy of Fe films prepared on vicinal Au(001) surfaces with different step orientations

2002 J. Phys.: Condens. Matter 14 8947

(http://iopscience.iop.org/0953-8984/14/39/304)

INSTITUTE OF PHYSICS PUBLISHING JOURNAL OF PHYSICS: CONDENSED MATTER

J. Phys.: Condens. Matter **14** (2002) 8947–8953 PII: S0953-8984(02)38194-3

Non-monotonic step-induced magnetic anisotropy of Fe films prepared on vicinal Au(001) surfaces with different step orientations

M Rickart, S O Demokritov and B Hillebrands

Fachbereich Physik and Forschungs- und Entwicklungsschwerpunkt Materialwissenschaften, Universität Kaiserslautern, D-67663 Kaiserslautern, Germany

Received 14 June 2002
Published 19 September 2002
Online at stacks.iop.org/JPhysCM/14/8947

Abstract

We report on investigations of the crystallographic structure and the magnetic anisotropies of epitaxial Fe films deposited on vicinal Au(001) surfaces for two miscut directions and various miscut angles. The stepped surface generates a uniaxial in-plane anisotropy contribution in addition to the fourfold anisotropy characteristic for Fe(001). With the step edges perpendicular to $[100]_{Fe}$ the uniaxial anisotropy constant is a non-monotonic function of the vicinal angle. At low vicinal angles the easy magnetization axis is parallel to the step edges. The effective uniaxial anisotropy constant first increases and then decreases for increasing vicinal angle, crossing zero at about $1.3^\circ \pm 0.2^\circ$. For higher angles the easy axis is perpendicular to the step edges. For the step edges perpendicular to $[110]_{Fe}$ the step-induced in-plane uniaxial anisotropy increases approximately linearly with the vicinal angle.

Magnetocrystalline anisotropies of ultrathin ferromagnetic films play a key role in the design of new materials for applications in research and technology. The break of lattice symmetry at the surface generates uniaxial magnetic anisotropy contributions which do not exist in the bulk [1, 2]. In particular, periodically stepped surfaces exhibit a uniaxial in-plane anisotropy due to a reduction of translational symmetry at the surface [3–5]. Investigations on bcc Fe films grown on stepped fcc Ag(001) or bcc W(001) single crystals with step edges parallel to $[100]_{Fe}$ revealed a quadratic dependence of the step-induced anisotropy constant on the vicinal angle [6, 7]. On the other hand, the uniaxial in-plane anisotropy in fcc Co/stepped Cu(001) depends linearly on the step density which is proportional to the vicinal angle [8]. Recently, Elmers and co-workers [9] found a correlation of morphology and magnetism of Fe grown on vicinal W[110] surfaces depending on the step orientation. Two main mechanisms are believed to give rise to the step-induced uniaxial anisotropy: the missing bonds of atoms at the surface (Néel's mechanism) and strain within the film [10]. In many cases a study of the dependence of the effective anisotropy strength on the film thickness d helps to determine the

surface contribution to the anisotropy, since the $1/d$ dependence of the anisotropy strength is a characteristic feature of surface anisotropies [11]. If the strain in the film does not depend on the thickness, a separation of the anisotropy into terms that are constant and inversely proportional to the thickness yields directly the volume and surface anisotropy contributions. But also magnetoelastic effects due to strain in the film yield anisotropy contributions which have to be considered as a thickness-dependent bulk property [12]. In this paper we report on a study of the step-induced uniaxial in-plane anisotropy as a function of the step density for the Fe/Au(001) system with the average orientation of step edges perpendicular to the $[100]_{Fe}$ as well as to the $[110]_{Fe}$ direction. We show that for one orientation of the steps the surface anisotropy contribution changes its sign with increasing vicinal angle. The volume uniaxial anisotropy constant shows different dependences on the vicinal angle for the miscut orientations studied.

Bulk metal single crystals, miscut at a small angle or polished with a continuous curvature with only one miscut orientation, were mainly used as substrates for studies of magnetic anisotropies of vicinal films [4, 6–9]. Metallic single crystals generally have a high crystalline quality, but for technological applications they are not very suitable as substrates, since they are difficult to manufacture, expensive, and tricky to handle. Therefore the use of semiconducting or insulating substrates is desirable [14, 15]. The Fe films studied in this work were grown on vicinal MgO(001) substrates covered with an Au buffer layer. All samples were prepared in an ultrahigh-vacuum (UHV) multi-chamber molecular-beam epitaxy system. The films were deposited by electron-beam evaporation onto the vicinal MgO(001) substrates (vicinal miscut angle between 0.5° and 7°) with deposition rates between 0.01 and 0.1 nm s^{-1} as monitored by a quartz microbalance. The analysis of the surface morphology and the sample structure was performed by means of low-energy electron diffraction (LEED), reflection high-energy electron diffraction, and scanning tunnelling microscopy (STM). STM was carried out with a commercial Park Scientific Instruments Autoprobe VP 2 UHV device. In order to remove the carbon contamination from the MgO surface and also to smooth the surface for improved growth of the subsequent metallic layers, the substrates were treated with a low-energy atomic oxygen ion beam at room temperature, as described in detail elsewhere [13]. Surfaces were judged clean if the Auger analysis with a sensitivity of better than 0.01 ML detected no remaining carbon contamination. Epitaxially grown Au buffers on MgO surfaces vicinal to (001) were used as the bases for the preparation of ultrathin bcc Fe films. MgO(001) with its lattice spacing of 0.421 nm is a good substrate for epitaxial growth of fcc Au(001) films (lattice constant 0.408 nm). Au films with a thickness of 150 nm were grown on MgO at a deposition rate of 0.1 nm s^{-1} and a substrate temperature of 120 °C. A thin seed Fe layer with a thickness of 1 nm was used to improve the growth of the buffer. The average orientation of the steps on the buffer surface corresponds to the miscut orientation of MgO. Similarly to in our earlier studies [14], the miscut angle obtained for the Au buffer surface differs slightly from that of the MgO surface due to a small difference between the layer-to-layer distances of Au(001) and MgO(001). Figure 1(a) shows a STM image of a 4° vicinal Au(001) surface with the miscut orientation along the $[100]_{Au}$ direction. The average orientation of the steps is still perpendicular to the $[100]_{Au}$ direction, although the step edges run alternately along $[110]_{Au}$ and $[1\bar{1}0]_{Au}$ forming a zigzag-shaped pattern. For the average orientation of the step edges perpendicular to the $[110]_{Au}$ direction of a 4° miscut sample, monatomic steps are observed as shown in figure 1(b). Fe(001) grows in the bcc phase with a 45° rotation of its lattice about the film normal on fcc Au(001) with a corresponding in-plane lattice mismatch of less than 1% [16, 17]. The step edges of the Au(001) surface perpendicular to the $[110]_{Au}$ direction correspond to step edges perpendicular to the $[100]_{Fe}$ direction of the Fe film. Thus, using the above buffers, two types of vicinal Fe film have been produced:

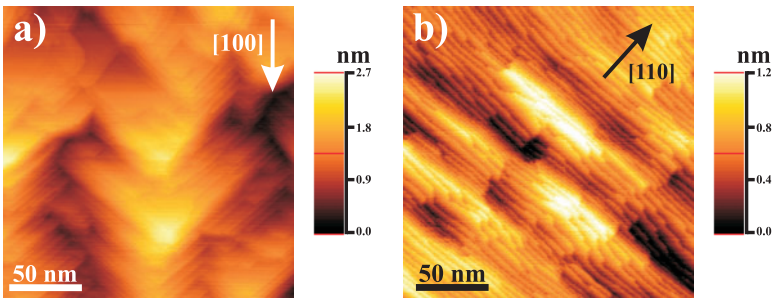

Figure 1. (a) A STM image of a vicinal Au layer with a nominally miscut angle of 4° along the $[100]_{\mathrm{Au}}$ direction. (b) A STM image of a 4° vicinal Au layer demonstrating monatomic steps perpendicular to the miscut orientation $[110]_{\mathrm{Au}}$.

(This figure is in colour only in the electronic version)

(i) with the average orientation of step edges perpendicular to $[100]_{\mathrm{Fe}}$;
(ii) with the average orientation of step edges perpendicular to $[110]_{\mathrm{Fe}}$.

The magnetic anisotropies of the Fe films were derived at room temperature from the frequencies of spin waves determined by means of Brillouin light scattering spectroscopy (BLS) [18, 19] and the evaluation of hysteresis loops obtained with the magneto-optical Kerr effect (MOKE) [20]. In both cases a focused laser beam was used as a probe. The Fe films were grown in the shape of a wedge, having the advantage that a large range of Fe thicknesses from 0.7 to 8 nm is available on one single sample by scanning the laser beam along the wedge. Due to the extremely small slope of the wedge (typically 0.66 nm mm^{-1}), the wedge shape of the Fe films does not influence the results obtained.

The total magnetic anisotropy energy density of a vicinal (001) film can be expressed by

$$E_{Ani} = K^{(2)}_{s,eff} \cos^2\theta + K^{(4)}_{p,eff} \sin^4\theta \cos^2\varphi \sin^2\varphi + K^{(2)}_{p,eff} \sin^2\theta \sin^2(\varphi - \varphi_0) \quad (1)$$

where $K^{(2)}_{s,eff}$, $K^{(2)}_{p,eff}$, and $K^{(4)}_{p,eff}$ are the effective constants of out-of-plane and in-plane uniaxial and in-plane fourfold anisotropy contributions with the attribute 'effective' indicating that at this stage no separation in volume and interface contribution has been made; θ and φ are the polar and the azimuthal angles of the magnetization, and φ_0 (together with the sign of $K^{(2)}_{p,eff}$) determines the orientation of the uniaxial in-plane easy axis with respect to the $[010]_{\mathrm{Fe}}$ axis. Thus, for $\varphi_0 = 0$ and $K^{(2)}_{p,eff} > 0$ the uniaxial easy axis coincides with $[010]_{\mathrm{Fe}}$, which is one of the easy axes of the fourfold anisotropy. In fact, all anisotropy constants can be determined by fitting the spin-wave frequencies measured as a function of the in-plane angle of the applied external field H [14, 21]. In this paper we will concentrate on the uniaxial in-plane anisotropy $K^{(2)}_{p,eff}$.

The second method for the determination of $K^{(2)}_{p,eff}$ is to measure static magnetization hysteresis loops with the magnetic field applied perpendicular to the easy axis [20]. This technique, however, becomes very insensitive if the easy axis of the induced anisotropy does not coincide with those of the strong fourfold anisotropy of Fe ($[100]_{\mathrm{Fe}}$ or $[010]_{\mathrm{Fe}}$). This is the case for the samples with the average orientation of step edges perpendicular to $[110]_{\mathrm{Fe}}$. For these samples, only BLS was used for the determination of $K^{(2)}_{p,eff}$. For the average orientation of step edges perpendicular to $[100]_{\mathrm{Fe}}$, the two techniques have provided the same results within their error margins: the easy axis of the induced uniaxial anisotropy is either parallel or perpendicular to the steps, depending on the miscut angle, i.e. $\varphi_0 = 0$ and $K^{(2)}_{p,eff}$ is either

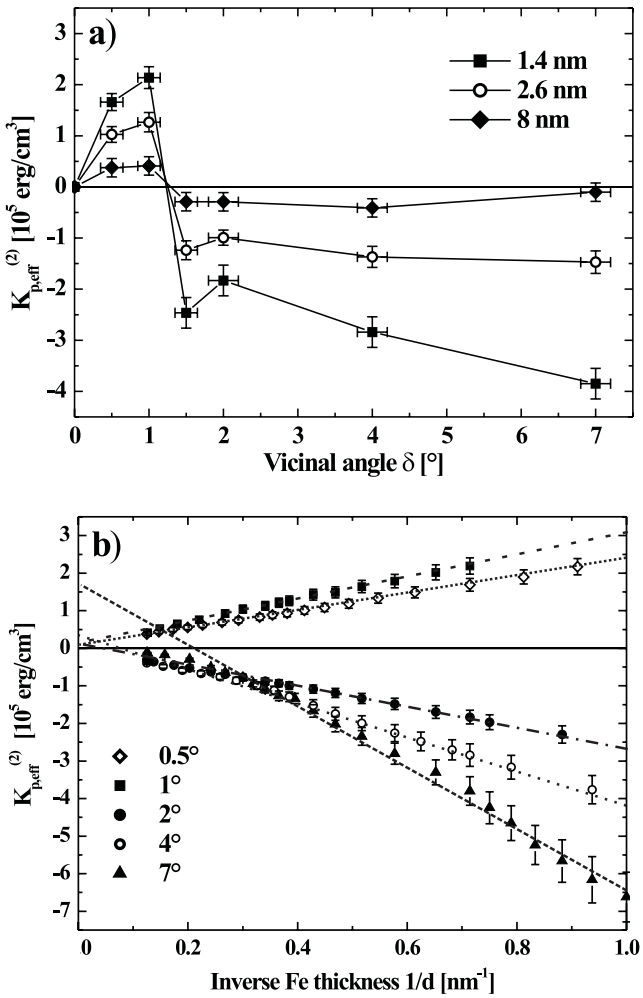

Figure 2. (a) $K_{p,eff}^{(2)}$ versus the vicinal miscut angle of the MgO(001) substrates for different Fe thicknesses. Positive (negative) values of $K_{p,eff}^{(2)}$ indicate an easy axis parallel (perpendicular) to the step edges. (b) $K_{p,eff}^{(2)}$ versus the Fe thickness as a function of $1/d$ for a film with the miscut in the $[100]_{\mathrm{Fe}}$ direction. The dashed curves indicate a linear fit according to $K_{p,eff}^{(2)} = K_p^{(2)} + 2k_p^{(2)}/d$. For 0.5° and 1° the easy axis is found to be parallel to the step edges; for higher vicinal angles the easy axis is perpendicular to the step edges.

positive or negative. Figure 2(a), showing $K_{p,eff}^{(2)}$ as a function of the vicinal miscut angle for different thicknesses of the Fe films, illustrates this. For small miscut angles $K_{p,eff}^{(2)}$ is positive and its value first increases, reaches its maximum, and then decreases, crossing zero at the critical miscut angle $\delta_c = 1.3° \pm 0.2°$, which is almost independent of the film thickness. For higher miscut angles $K_{p,eff}^{(2)}$ becomes negative and decreases with δ for small Fe film thicknesses.

Before we discuss the origin of the step-induced anisotropy, the use of equation (1), which implies the uniform magnetization of the film, and of the coherent rotation remagnetization scenario should be validated. In fact, for the BLS measurements the determination of the

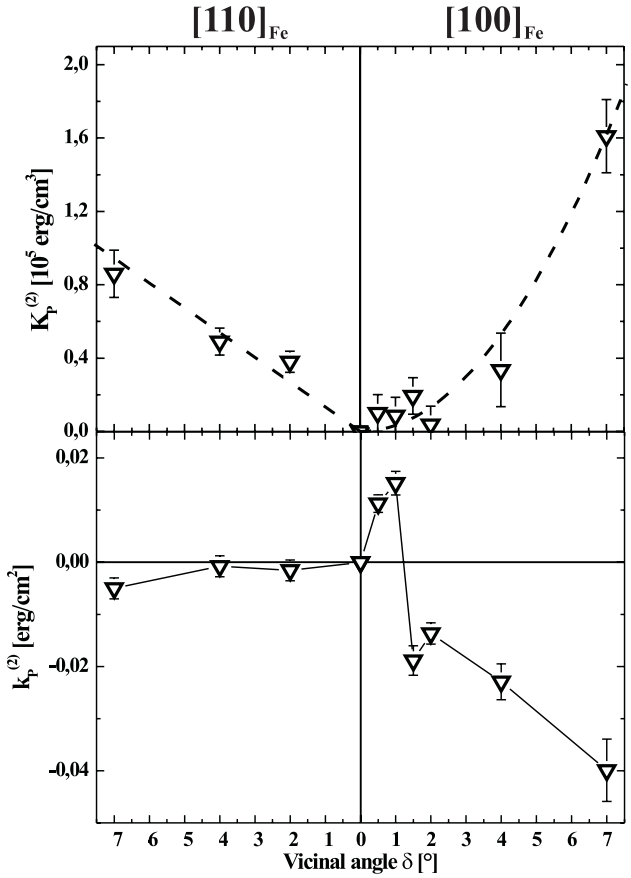

Figure 3. Surface ($k_p^{(2)}$) and volume ($K_p^{(2)}$) contributions of the uniaxial in-plane anisotropy versus the vicinal angle of the MgO(001) substrates. The left and the right panel correspond to the films with average orientation of step edges perpendicular to $[110]_{\mathrm{Fe}}$ and $[100]_{\mathrm{Fe}}$, respectively. The dashed curves depict the behaviour of $K_p^{(2)}$: linear dependence on the vicinal angle for $[110]_{\mathrm{Fe}}$ and quadratic for $[100]_{\mathrm{Fe}}$ orientation.

anisotropy constants is independent of the remagnetization scenario proposed, because the samples were probed while magnetically saturated. For the hysteresis loop investigations, many possibilities for magnetization switching exist [5, 22]. However, for the values of the exchange constant $J = 2 \times 10^{-6}$ erg cm^{-1}, $K_p^{(4)} = 4.7 \times 10^5$ erg cm^{-3}, and the uniaxial in-plane anisotropy $K_{p,eff}^{(2)}$ in the range of -6.5×10^5–2.5×10^5 erg cm^{-3} obtained from our data, the comparison with the analysis performed in [5] demonstrates that a nearly coherent rotation dominates the remagnetization process.

To investigate the induced anisotropy in detail, the dependence of $K_{p,eff}^{(2)}$ on the Fe film thickness was studied. It is presented in figure 2(b) as a function of $1/d$ for films with a miscut along the $[100]_{\mathrm{Fe}}$ direction. For small miscut angles the measured dependence can be fitted by the usual expression $K_{p,eff}^{(2)} = K_p^{(2)} + 2k_p^{(2)}/d$, where K_p and k_p describe the volume and surface contributions, respectively. A possible effect from relaxing strain on the step-induced anisotropy should be considered in general. However, the data in figure 2(b) for the miscut angle $\delta < 7^\circ$ appear linear, implying that the change of the strain is not significant for the

miscut angles used and the interval of Fe thicknesses. Thus, for those data the separation of $K^{(2)}_{p,eff}$ into $K^{(2)}_p$ and $k^{(2)}_p$ is validated. For $\delta = 7°$ a deviation from the linear dependence is seen for $d > 3$ nm. The effect is apparently connected with the onset of the stress relaxation in the growing Fe film. The linear fit for the separation of $K^{(2)}_p$ and $k^{(2)}_p$ was then performed for Fe thicknesses $d < 3$ nm.

The dependences of $K^{(2)}_p$ and $k^{(2)}_p$ on the miscut angle obtained are presented in figure 3 for both of the orientations of the steps that were investigated. For the Fe films with the average orientation of step edges perpendicular to the $[110]_{\mathrm{Fe}}$ direction, $K^{(2)}_p$ increases proportionally to the miscut angle (i.e. the step density) indicating a linearly growing stress in the bulk of the films. The interface contribution $k^{(2)}_p$ is negligible. The zigzag-shaped steps with the average distribution perpendicular to $[110]_{\mathrm{Fe}}$ locally consist of step edges along $[100]_{\mathrm{Fe}}$ and $[010]_{\mathrm{Fe}}$. Averaging of these two anisotropy contributions along $[100]_{\mathrm{Fe}}$ and $[010]_{\mathrm{Fe}}$ would explain the vanishing interface contribution. The volume contribution is not cancelled out since the bulk properties of a thick vicinal film are mainly determined by the average crystallographic orientation of its surfaces. For another orientation of steps (perpendicular to $[100]_{\mathrm{Fe}}$) $K^{(2)}_p$ is roughly proportional to δ^2. $k^{(2)}_p$ demonstrates the change of its sign in a profound way, indicating the surface nature of the non-monotonic behaviour of $K^{(2)}_{p,eff}$. We connect the non-monotonic dependence of $k^{(2)}_p$ on the miscut angle with essential changes of the surface morphology near $\delta_c = 1.3° \pm 0.2°$. It was clearly observed for the samples with the average orientation of step edges perpendicular to $[100]_{\mathrm{Fe}}$ using LEED and STM. The detailed study will be published elsewhere [23].

To achieve an understanding of the observed anisotropy phenomena, numerical calculations are necessary; these are, however, outside the scope of this work. From our work it is evident that two origins of strain must be properly taken into account. First, due to the in-plane mismatch of 1%, a misfit dislocation network, probably located at the interface steps, is formed to release the misfit strain. Second, a perpendicular misfit of 42% exists at each step. It cannot be released by dislocations. Instead, it is accommodated by the Fe film, and it decreases with distance from the interface. The two strain sources might show an interplay which determines the local strain at the atoms close to each step. The present work might serve to guide numerical simulations to uncover the details of strain relaxation under these combined mechanisms.

Acknowledgments

Support by the Deutsche Forschungsgemeinschaft and the European Science Foundation programme NANOMAG is gratefully acknowledged.

References

[1] Heinrich B, Urquhart K B, Arrott A S, Cochran J F, Myrtle K and Purcell S T 1987 *Phys. Rev. Lett.* **59** 1756
[2] Schulz B and Baberschke K 1992 *Phys. Rev.* B **50** 13 467
[3] Berger A, Linke U and Oepen H P 1992 *Phys. Rev. Lett.* **68** 839
[4] Chen J and Erskine J L 1992 *Phys. Rev. Lett.* **68** 1212
[5] Hyman R A, Zangwill A and Stiles M D 1998 *Phys. Rev.* B **58** 9276
[6] Kawakami R K, Escorcia-Aparicio E J and Qiu Z Q 1996 *Phys. Rev. Lett.* **77** 2570
[7] Choi H J, Qiu Z Q, Pearson J, Jiang J S, Li D and Bader S D 1998 *Phys. Rev.* B **57** R12 713
[8] Kawakami R K, Bowen M O, Choi H J, Escorcia-Aparicio E J and Qiu Z Q 1998 *Phys. Rev.* B **58** R5924
[9] Elmers H J, Hausschild J and Gradmann U 2000 *J. Magn. Magn. Mater.* **221** 219
[10] Chuang D S, Ballentine C A and O'Handley R C 1994 *Phys. Rev.* B **49** 15 084
[11] Néel M L 1954 *J. Physique Radium* **15** 376
[12] Shick A B, Gornostyrev Yu N and Freeman A J 1999 *Phys. Rev.* B **60** 3029

[13] Rickart M, Roos B F P, Mewes T, Jorzick J, Demokritov S O and Hillebrands B 2001 *Surf. Sci.* **495** 68
[14] Frank A R, Jorzick J, Rickart M, Bauer M, Fassbender J, Demokritov S O, Hillebrands B, Scheib M, Keen A, Petukhov A, Kirilyuk A and Rasing Th 2000 *J. Appl. Phys.* **87** 6092
[15] Leeb T, Brockmann M, Bensch F, Miethaner S and Bayreuther G 1999 *J. Appl. Phys.* **85** 4964
[16] Grünberg P, Demokritov S, Fuss A, Schreiber R, Wolf J A and Purcell S T 1995 *J. Magn. Magn. Mater.* **104–107** 1734
[17] Krebs J J, Jonker B T and Prinz G A 1987 *J. Appl. Phys.* **61** 2596
[18] Demokritov S and Tsymbal E 1994 *J. Phys.: Condens. Matter* **6** 7145
[19] Hillebrands B 1999 *Brillouin Light Scattering in Solids VII (Springer Topics in Applied Physics vol 75)* ed M Cardona and G Güntherodt (Berlin: Springer) p 174
[20] Weber W, Allenspach R and Bischof A 1997 *Appl. Phys. Lett.* **70** 520
[21] Hillebrands B 1990 *Phys. Rev.* B **41** 530
[22] Hyman R A, Zangwill A and Stiles M D 1999 *Phys. Rev.* B **60** 14 830
[23] Rickart M *et al* 2002 at press